Jour. Fac. Sci., Hokkaido Univ., Ser. IV,
vol. 22, no. 4, Aug., 1990, pp. 591-609.

PALEOMAGNETISM OF THE NORTHWESTERN PART OF THE MAHABHARAT SYNCLINORIUM, LESSER HIMALAYA, NEPAL

by

Pitambar Gautam*

(with 13 text-figures and 5 tables)

Abstract

Remanent magnetization of the low-grade metasediments (272 specimens/131 samples from 26 sites), which constitute the Nawakot and Kathmandu Complexes in the northwestern part of the Mahabharat synclinorium, is described. Alternating field (AF) and thermal (TH) demagnetization experiments reveal stable secondary magnetization resting in hematite and represented by normal and reverse polarities. The secondary remanence is of prefolding origin in the rocks from the Nawakot Complex while it post-dates major folding in those from the Kathmandu Complex. The directions are consistent with near-equatorial shallow paleolatitudes. The secondary remanence is interpreted to indicate the occurrence of a series of events, i. e. reheating and/or metamorphism, nappe emplacement and folding in this area at the onset or shortly after the early Eocene India-Eurasia collision.

Introduction

Paleomagnetic research in orogenic belts has shown that the rocks exhibit multi-component or multi-phase remanent magnetization. Apart from the primary magnetization component, the magnetic remanence records the secondary effects (e. g., oxidation, mild or intense reheating, low-grade metamorphism through burial, deformation or igneous intrusion) which the rocks have experienced during their history. The secondary magnetizations may be of viscous, thermal, chemical or mixed (thermochemical, thermoviscous etc.) origin. In general, the occurrence of multi-component remanences is more common in older rocks because of greater probability of exposure to one or more thermal, chemical or tectonic events. In metamorphic rocks, the primary magnetization may be completely overprinted by secondary remanence which may rest on a new mineral phase produced during the metamorphism. Studies of the secondary componets, therefore, may provide information on the timing of the metamorphism and associated tectonic events.

This work is an attempt to elucidate the nature of magnetization in the low-grade metamorphic rocks of the Nawakot Complex and the unmetamorphosed to metamorphosed- up to -biotite grade sediments of the Kathmandu Complex in the

---

Contribution from the Department of Geology and Mineralogy, Faculty of Science, Hokkaido University, No. 1999

* Presently at: Central Department of Geology, Tribhuvan University, Kirtipur, Kathmandu, Nepal.

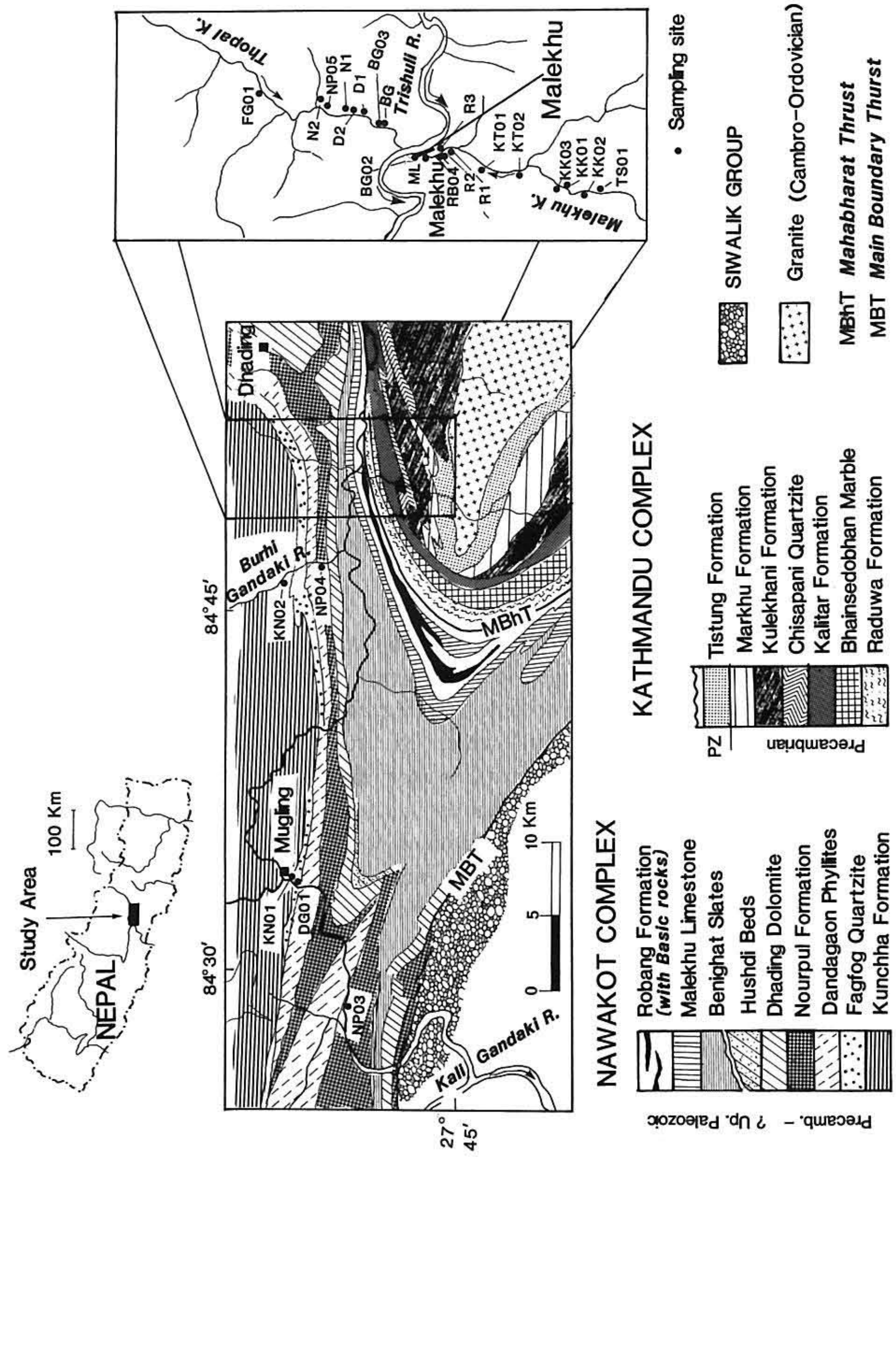

Text-fig. 1 Geologic map showing the main lithological divisions in the northwestern part of the Mahabharat Synclinorium (after Stöcklin & Bhattarai, 1980) and the paleomagnetic sampling sites.

Lesser Himalaya. The remanent magnetization properties are discussed in detail and interpretation of the components is given. Part of the material described has been taken from Gautam and Yoshida (1988).

Geologic setting, sampling and laboratory procedure

The area dealt with forms a part of 'the Kathmandu area and Central Mahabharat range' (Stöcklin and Bhattarai, 1980; Stöcklin, 1980). Two major rock assemblages are recognized: i) the Kathmandu Complex -a part of the Lesser Himalayan crystallines consisting of relatively high-grade metasediments (up to garnetiferous schists) but also including unmetamorphic or weakly metamorphosed sediments having fossils of early-Middle Paleozoic age on top and containing granites and gneisses, and ii) the Nawakot Complex -a part of the Lesser Himalayan sediments consisting almost exclusively of low-grade (sericite-chlorite) metasediments. A major discordance known as the Mahabharat Thrust (MBhT) separates the two groups. The Kathmandu Complex and Nawakot Complex constitute the core and peripheral part of the WNW-ESE trending structure-Mahabharat synclinorium, respectively.

Sampling of the rocks was restricted to three routes (Text-fig. 1): the Thopal and Malekhu Khola route in the vicinity of Malekhu (27.8°N, 84.8°E) sampled in detail; the Burhi Gandaki route; and, the Mugling-Narayanghat road section. In addition, crinoidal limestone samples were collected from a site in the Phulchowki hills, a well known fossil locality, south of Kathmandu. Samples were collected from road cut and river bank exposures. Seventy eight samples from 19 sites belong to the Nawakot Complex and 53 samples forming 7 sites are from the Kathmandu Complex. Block sampling and *in situ* drilling methods were applied. The total number of specimens (2.54 cm diameter, 2.2 cm length) for Nawakot Complex and Kathmandu Complex are 134 and 138, respectively.

Laboratory procedure is essentially the same as described in Gautam (1989). NRM measurements were followed by AF and TH demagnetization experiments and component-analysis was carried out. Thermomagnetic analysis and isothermal remanent magnetization (IRM) acquisition experiments were performed in order to determine the magnetic minerals.

Remanent magnetization in the Nawakot Complex rocks

NRM data

Table 1 shows the NRM intensities and directions. Black slates, calcareous sediments and some phyllitic rocks possess very weak intensities (n. 10^{-4} to n. 10^{-5} A/m) and their directions cannot be determined with reliability. For the rest of the lithologies, the intensities range between n. 10^{-4} and n. 10^{-1} A/m. Hematite schists are the strongest (n. 10^{-1} A/m) followed by the metasandstones of Nourpul Formation (n. 10^{-2} A/m).

Table 1 Natural remanent magnetization intensities and site-mean directions from the Nawakot Complex with sampling details

Site	N (n)	Intensity (x10^{-4} A/m)			Mean Direction				lithology	Attitude
		Mean		S	D (deg.)	I (deg.)	K	α_{95} (deg.)		Strike/Dip
a) *Upper Nawakot Group :*										
/Robang Fm. (R, BG), Malekhu Limestone (ML) and Benighat Slates (BG)/										
R1	16 (8)	5,371.1	±	2,548.0	240	25	2	30.3	hematite schist	68/ 84S
R2	9 (4)	26.1	+	43.6	202	−22	3	27.2	ph. /amphibolite	73/ 73S
R3	3 (3)	10.6	+	9.6	—	—	—	—	chloritic ph.	70/ 75S
RB04	7 (7)	75.9	±	105.1	—	—	—	—	amphibolite	80/ 85S
ML	2 (2)	1.3		—	—	—	—	—	fine-cryst. limestone	85/ 98S*
BG	7 (3)	8.5	±	4.0	3	73	63	6.7	quartzose sl.	94/ 95S*
BG02	6 (6)	0.9	±	0.7	—	—	—	—	black carb. sl.	95/ 75S
BG03	5 (4)	8.1	±	5.6	—	—	—	—	quartzose sl.	94/ 87-106S*
b) *Lower Nawakot Group :*										
/Dhading Dolomite (D), Nourpul Fm. (N, NP), Dandagaon Phyllite (DG), Fagfog Quartzite (FG) and Kunchha Fm. (KN)/										
D1	6 (3)	2.9	±	4.0	360	44	77	6.5	sparry dolomite	108/ 90S
D2	2 (2)	0.4	±	0.0	—	—	—	—	dolomite	92/115S*
N1	10 (3)	123.0	±	48.1	98	−44	4	22.3	semi-pelitic ph.	92/ 95S*
N2	8 (3)	408.7	±	781.0	97	−45	36	8.3	quartz ph.	92/115S*
NP03	3 (3)	4,384.3	±	4,176.4	—	—	—	—	hematite schist	255/ 45N
NP04	14 (5)	493.5	±	329.3	349	6	6	15.3	quartzose ph.	90/122S*
NP05	8 (8)	85.2	±	50.3	—	—	—	—	quartzose ph.	110/115S*
DG01	10 (3)	335.8	±	328.9	—	—	—	—	phyllitic ss.	70/ 80S
FG01	5 (5)	0.3	±	0.8	—	—	—	—	chloritic ph.	85/110S*
KN01	6 (3)	1.5	±	1.4	—	—	—	—	sl.	60/ 78S
KN02	7 (3)	14.4	±	12.2	—	—	—	—	sl.	67/120S*

Note:

1. *Symbols* : N : no. of specimens ; n : no. of samples ; S : standard deviation of mean intensity ; D : declination ; I : inclination ; K : estimate of the precision parameter ; α_{95} : radius of 95% confidence circle.
   Mean directions and the statistical parameters are ater Fisher (1953) with unit weight to specimens. Directions are *in situ.* Mean directions with $\alpha_{95}>30°$ are not presented because they have no practical significance.
2. *Abbreviations* : ss.=sandstone, carb.=carbonaceous, sl.=slate, ph.=phyllite.
3. Attitudes followed by asterisk are for overturned beds.
4. Mean directions with $\alpha_{95}>30°$ are assumed to have no significance and are not listed.
5. Part of the data is taken from Gautam and Yoshida (1988)

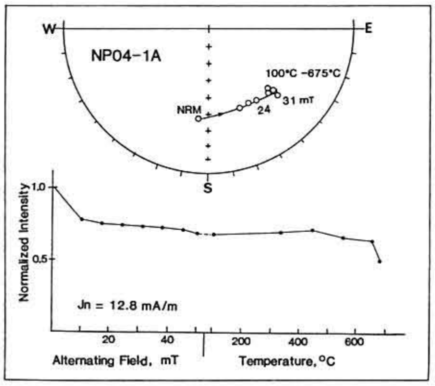

Text-fig. 2 Af-followed-TH demagnetization response of a specimen from site NP04.

a. Vector migration plot (upper diagram) showing changes in direction of the remanent magnetization vector during successive demagnetization. Open (solid) circles denote upward (downward) inclinations and represent projections in equal-area net.

b. Normalized intensity decay curve (lower diagram) to show the changes in intensity during demagnetization. Jn is the initial NRM intensity.

Demagnetization behavior

In several instances, AF demagnetization up to 50-53 mT effectively removes the soft components leading to stable directions which remain stable up to high temperatures during further thermal demagnetization as shown previously (Gautam and Yoshida, 1988). Additional data (Text-fig. 2) clearly support this fact. In some cases, however, pronounced variation in the magnetic behavior between samples was observed (Text-fig. 3). In the latter case, the presence of antipodal shallow NNE and SSW directions can be inferred, although due to a few numbers of specimens no accurate estimates of the directions could be obtained.

Mean directions at site level and the associated statistical parameters calculated according to Fisher (1953) are given in Table 2.

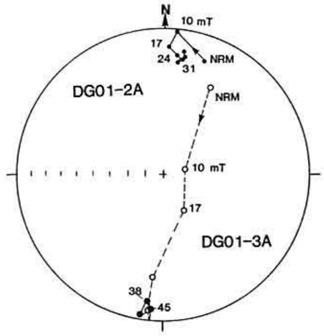

Text-fig. 3 Vector migration plots to show the dual polarity behavior of specimens from Dandagaon Formation.

Table 2 Summary of magnetic components from the rocks of Nawakot Complex

Site	N(n)	Peak demagnetization field or range	Mean Direction						Polarity (N/R)
			In Situ / / Tilt-corrected						
			(deg.)	I / / (deg.)	D (deg.)	I (deg.)	k	α_{95} (deg.)	
a) *Characteristic component* :									
R1	3	30 mT	234	34	212	− 9	64	10	R
BG	3	53 mT	327	70	196	10	116	7	R
N1	3	30 mT	96	−50	41	1	123	7	N
N2	3	50 mT	134	−61	26	7	44	12	N
NP04	6/5	40 mT	110	−23	60	− 3	170	5	N
NP05	6/8	50 mT	107	−53	60	21	93	7	N
i) Mean of N & NP sites, only :									
	(N=4)		110	−47.5	47	6.7			
		(k_1=18, $\alpha 1_{95}$=22.1)			(k_2=18, $\alpha 2_{95}$=22.5)				
			Paleolatitude (°N)=3.3±11.3						
ii) Mean of all sites, N & R polarities included :									
	(N=6)				39	4.3	15	17.6	
			Paleolatitude (°N)=2.1±8.8						
b) *Soft components* :									
i) Recent									
D1	3	20 mT	0	43	—	—	81	8	N
N2	3	0-20 mT	7	51	—	—	17	19	N
ii) Similar to the characteristic component but of post-tiliting origin ?									
NP04	3/2	<53 mT	231	− 2	—	—	40	13	N
NP05	1/1	<53 mT ?	219	3	—	—	—	—	N

Note :

1 . A single number corresponds to the number of samples (n), where unit weight was given to samples. Otherwise, N is the number of specimens and n is the number of specimens, unit weight being given to specimens. N/R in the last column denote normal and reverse polarities, respectively.
2 . Part of the data is taken from Gautam & Yoshida (1988).
3 . Other conventions as in Table 1.

Remanent magnetization in the Kathmandu Complex rocks

NRM data

NRM intensity and site-mean directions are listed in Table 3. Micaceous sandstones from KK and TS sites possess very strong magnetic moments (n. 10^{-1} A/m) whereas the phyllitic slates and sandstones from KT sites possess intensities weak by an order of magnitude. The NRM directions for site KK show rather well-grouping. The crinoidal limestone samples are magnetically weak and the directions-totally random.

Table 3 Natural remanent magnetization intensities and site-mean directions from the Kathmandu Complex with sampling details*

Site	N (n)	Intensity ($x10^{-4}A/m$) Mean	S	Mean Direction D (deg.)	I (deg.)	K	α_{95} (deg.)	lithology	Attitude Strike/Dip
a) *Phulchauki Group*:									
/Phulchauki limestone (PP) and Tistung Formation (TS)/									
PP01	21(7)	6.9	± 3.8	—	—	—	—	red crinoidal ls.	230/65S
TS01	26(10)	6,775.7	±8,000.2	356	− 9	2	18.3	micaceous ss.	98/80N
b) *Bhimphedi Group*:									
/Kulekhani (KK) and Kalitar (KT) Formations/									
KK01	16(8)	4,022.7	±2,312.6	20	−26	54	4.8	light gray ss.	80/45-55S
KK02	16(7)	1,608.6	± 983.4	26	− 1	80	4.0	micaceous ss.	118/60S
KK03	13(7)	2,890.9	±2,257.1	—	—	—	—	micaceous ss.	93/55S
KT01	26(7)	289.3	± 515.2	348	46	4	14.4	phyllitic sl.	76/60S
KT02	21(7)	869.7	± 951.6	39	−10	10	10.0	micaceous ss.	250/88N

* For symbols and other conventions refer Table 1.

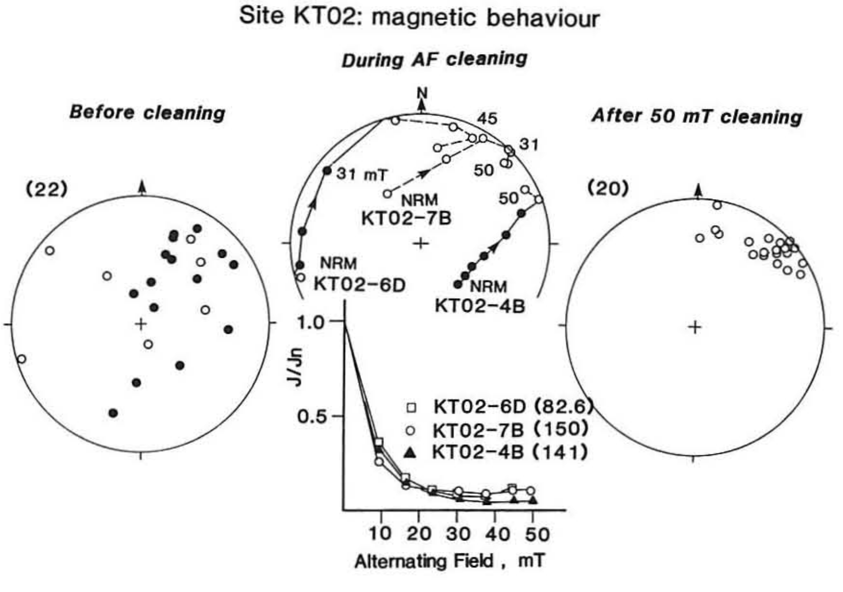

Text-fig. 4 Magnetic behavior of specimens from site KT02, Kalitar Formation. Left: equal-area plot of specimen NRM directions (solid and open circles denote downward and upward pointing directions, respectively). Centre: vector migration plots and intensity decay patterns. Right: equal-area plot of 'cleaned' vectors.

Demagnetization behavior

In general, AF demagnetization up to 50 mT is sufficient to remove soft component(s), if any, present in the specimens. The AF-treated specimens were found to be very stable up to high temperatures which are above 600℃ and sometimes

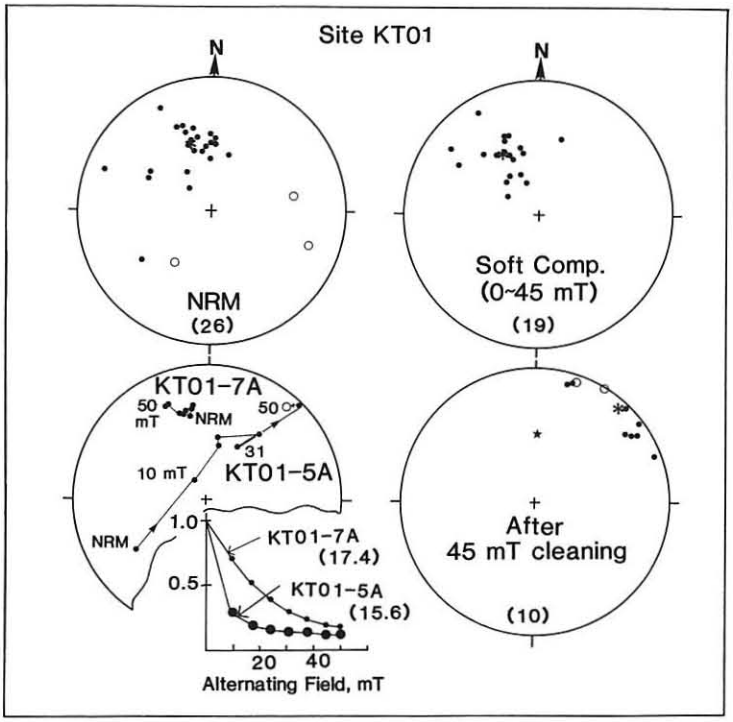

Text-fig. 5 Magnetic behavior of specimens from site KT01. Soft components were derived by least-square analysis of demagnetization data. Of the 26 initial specimens only 10 had reasonable intensities and relatively stable directions after demagnetization at 45mT. Star shows the present dipole field direction for Malekhu.

reach to 670-680℃. The contribution of components with soft coercivity is highly variable and so is the proportion of normal and reverse components when both coexist in a single specimen. A major fraction of the total NRM in the KT specimens is represented by unstable random direction. A steady convergence to shallow NNE or SSW components during the treatment is clear (Text-figs. 4 and 5). Coexisting normal and reverse polarity components were also found (Text-fig. 6). Ideal demagnetization response is exhibited by specimen KK02-1B in which after elimination of a minor reverse component, a stable direction is achieved as demonstrated by the exact convergence of the components in the vector plots (Text-fig. 7).

Site-mean directions are given in Table 4.

Magnetomineralogy

IRM acquisition curves are shown in Text-figs. 8 and 9. The curves can be broadly divided into two types: those exhibiting an early saturation and those in which no saturation is achieved. These curves demonstrate the presence of mag-

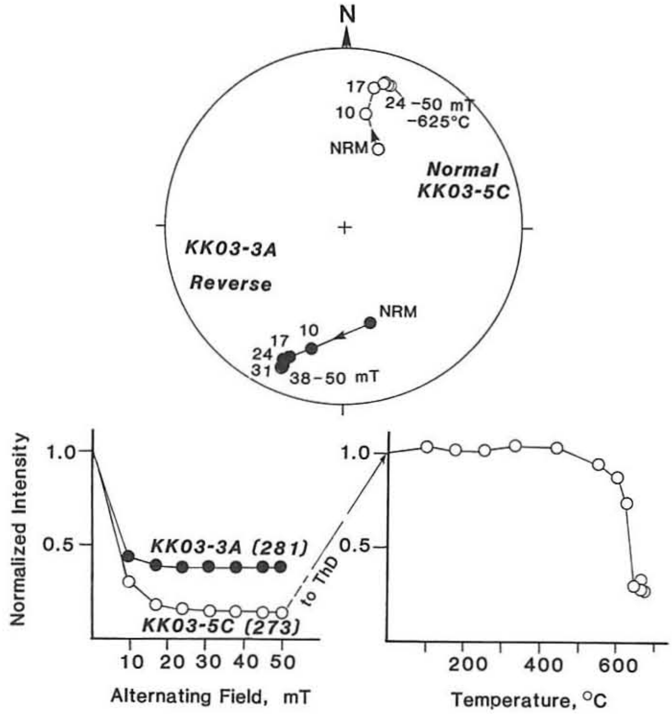

Text-fig. 6 Dual polarity nature of the stable direction as shown by demagnetization analysis of specimens from site KK03 (Kulekhani Formation). Upper diagram: vector migration plots; lower diagrams: intensity response curves.

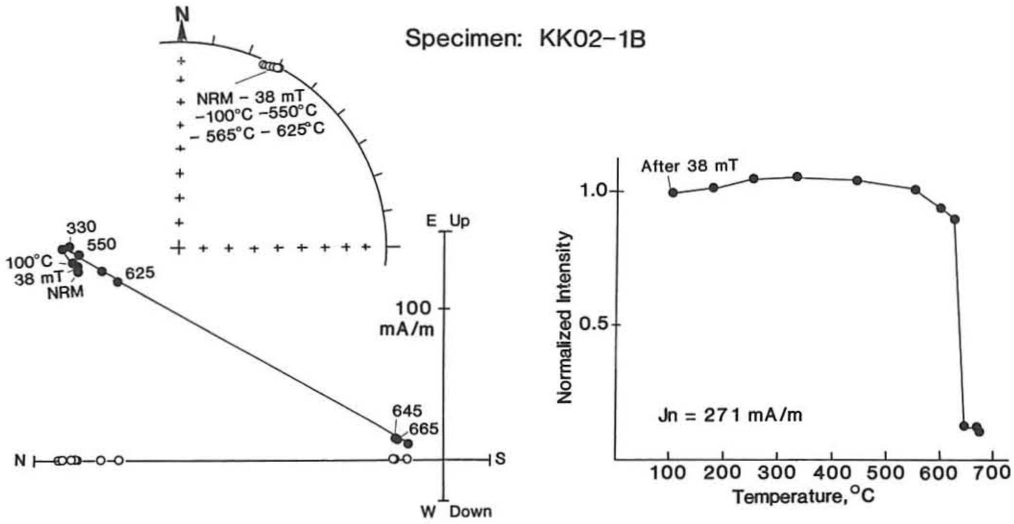

Text-fig. 7 AF-followed-TH demagnetization response of a specimen from site KK02 showing major blocking temperature range of 625-645℃. The lower figure in the left side represents orthogonal projection diagram (Zijderveld, 1967) where the projections of the end-points of the resultant vector during successive demagnetization are shown. Solid and open circles are the projections on the horizontal and N-S vertical planes, respectively.

Table 4 Summary of magnetic components from the rocks of Kathmandu Complex

Site	N/n	Demagnetization value or range	Mean direction D (deg.)	I (deg.)	k	α_{95} (deg.)	Polarity N/R
a) *Characteristic component*:							
TS01	7	45 mT	19	−7	41	8.2	N
	1	625–645℃	204	4	—	—	R
KK01	8	38m T	20	−26	96	5.0	N
KK02	7	50 mT	25	−1	205	3.7	N
KK03	3	38 mT	15	−3	13	22.2	N
	5	38 mT	202	11	35	10.6	R
KT01	10/4	43 mT	41	6	16	11.0	N
KT02	20/7	50 mT	40	−15	16	7.8	N
i) Mean directions: KK & TS							
N polarity, *in situ*:			20	−9	44	13.8	
		(Bedding corrected:	23	50	12	27.7)	
R polarity, *in situ*:			203	7	—	—	
N+R polarity, *in situ*:			21	−8.6	68	8.1	
Paleolatitude (°S) = −4.3±3.5							
ii) Overall mean: TS, KK & KT sites, *in situ*:							
N = 8			26	−7.7	36	9.4	
Paleolatitude (°S) = −3.8±4.7							
b) *Other components*:							
(Recent component and recent but deviated towards magnetic lineation axis)							
KT01	4(3)	<20 mT	3	49	49	10.0	N
KT01	19(7)	<45 mT	330	47	18	7.6	N

Note:

1. For TS and KK sites the mean directions were first calculated at sample level and then unit weight was given to sample means to calculate the site mean. For the KT sites unit weight was given to specimens.
2. Other conventions as before.

netic minerals with soft and hard coercivities represented by magnetite-group and hematite (Dunlop, 1972), respectively. The relative contribution of the soft and hard components can be roughly determined by measuring the remanent magnetization after demagnetization of the applied IRM in peak alternating field, say 50 mT, as shown for specimens NP04-5B and TS01-2C. The soft component carries the unstable low coercivity remanence while the hard one carries hard coercivity and high unblocking temperature remanence. The specimens which were largely dominated by the soft coercivity natural remanence showed only soft coercivity minerals during IRM acquisition.

Macroscopic and microscopic examination of the samples and the Curie temperature determinations suggest that hematite is ubiquitous in the rocks of the

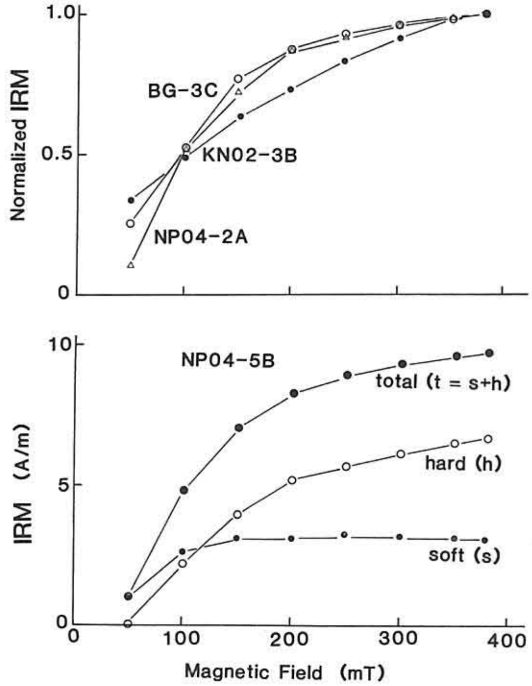

Text-fig. 8 Isothermal remanent magnetization acquisition curves for some specimens from the Nawakot Complex. Upper diagram: normalized intensity curves. Lower diagram; separation of the total intensity into soft and hard coercivity components.

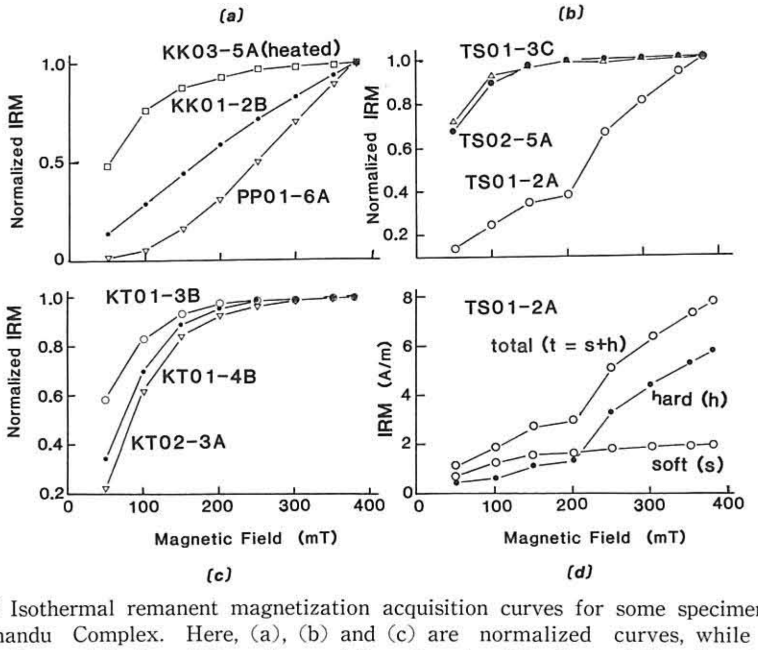

Text-fig. 9 Isothermal remanent magnetization acquisition curves for some specimens from the Kathmandu Complex. Here, (a), (b) and (c) are normalized curves, while (d) demonstrates the contribution of the soft coercivity mineral and hard coercivity mineral to the total IRM intensity of the specimen.

Kathmandu and Nawakot Complexes.

Interpretation of the directions

1. Timing of the remanence

a) Soft components

In a few cases, well-grouping of soft components was noted. The mean direction from site D1 and the softer component from site N2 are very close to the dipole field direction at present for Malekhu (I=47°). So these directions are interpreted to represent the recent field component of secondary origin. Similar soft components were observed in specimens from site BG and KT as well. In majority of specimens from site KT01, however, the mean declination is westerly deviated. This is believed due to the effect of magnetic anisotropy which is discussed elsewhere (Gautam, 1990).

b) Characteristic components

The stable components are designated as the characteristic derections as they are thought to represent the dominant part of the remanence in the rocks studied.

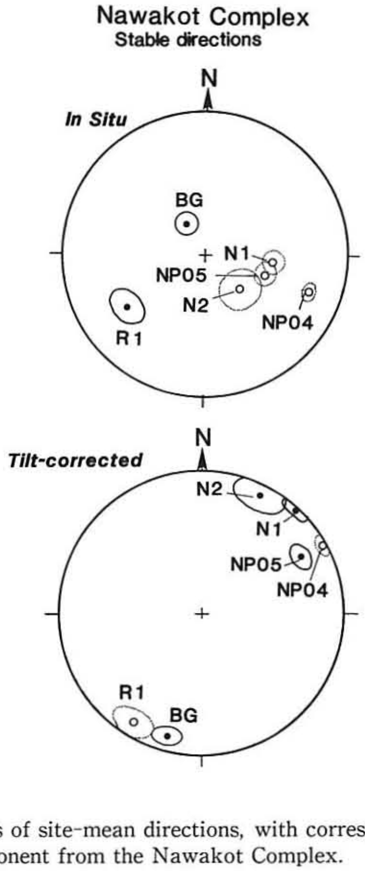

Text-fig. 10 Equal-area plots of site-mean directions, with corresponding ovals of 95% confidence, forming the stable component from the Nawakot Complex.

Site-mean directions from the Nawakot Complex are plotted in Text-fig. 10. A remarkable feature is that the stable (high coercivity range/high unblocking temperature) directions diverge into two roughly antipodal directions after tilt correction. These groups are assumed to represent normal and reverse polarities which probably record the ambient geomagnetic field in two polarity states acquired during a relatively long time span. Grouping of the directions forming roughly antipodal directions after tilt-correction is taken as an evidence for the pre-folding (at least, prior to major tilting) acquisition of the remanence. In some sites, e. g. NP04 and NP05, *in situ* components with southwesterly declination and shallow inclination were recognized from the demagnetized curves (Table 2, b(ii)). Such directions were probably acquired posterior to the major folding.

Site-mean directions from the Kathmandu Complex (Text-fig. 11) are well -grouped before tilt-correction in contrast to those from the Nawakot Complex. Moreover, they resemble to the tiltcorrected directions from the Nawakot Complex. This suggests that the directions with NNE or SSW declinations and shallow near-horizontal inclinations were acquired in the Kathmandu Complex rocks posterior to major tilting. Judging from the presence of both polarities, it is suggested that the magnetization process was active for a long period (several Myrs) during which at least once the geomagnetic field reversed its polarity.

High coercivity ranges/high unblocking temperatures of the remanence, IRM experiments and microscopic evidences suggest that the stable remanence rests on hematite, which is believed to be an authigenic product due to metamorphism. Hence, the magnetization owes to some thermo-chemical processes which took place at the time of metamorphism and it is certainly of secondary origin.

Interpretation of the components is attempted by comparing the inclinations with the inclinations to be expected in the area from the Indian APWP (Table 5).

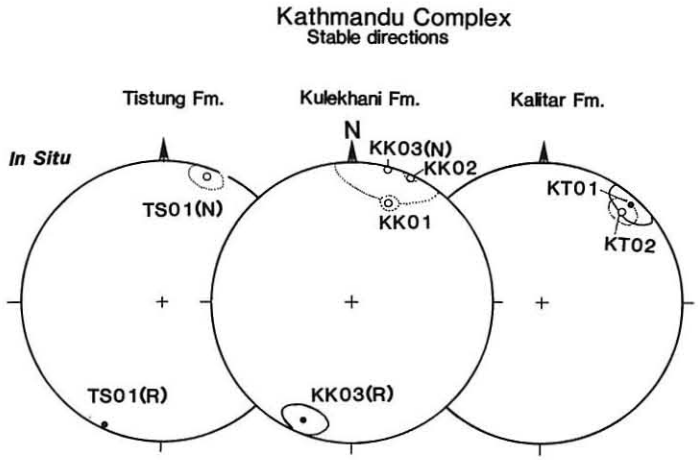

Text-fig. 11 Equal-area plots of site-mean directions, with corresponding ovals of 95% confidence, forming the stable directions from the Kathmandu Complex.

The upper section in Text-fig. 12 shows the paleolatitude vs. time plot for the location of Malekhu and the plots of paleolatitude estimates (stars) with vertical uncertainty bars in the paleolatitude curve. Although the mean paleolatitude value calculated from the tilt-corrected directions from the Nawakot Complex plots more northerly than the mean paleolatitude value derived from the *in situ* directions from the Kathmandu Complex, there is clearly an overlap and the former has larger uncertainties. Hence, the difference between the two estimates is interpreted to be statistically insignificant. At the same, greater significance is attached to the paleolatitude estimate from the Kathmandu Complex. From the above reasoning, the most likely time range of acquisition of the stable remanence would be around 50-55Ma, although the paleolatitude-time boxes cover a rather longer period ranging roughly from 35 to 57Ma.

2. Estimation of the amount of rotation

The discrepancy between the expected, from the Indian APWP, and observed declinations is interpreted in terms of the clockwise rotation of the Malekhu area

Table 5 Paleomagnetic directions and paleolatitudes expected for Malekhu (27.8°N, 84.8°E)

Details of APWP*				Parameters for Malekhu		
Age (Ma)	Anomaly no.	Pole lat. (°N)	Pole long. (°E)	Decl. (°E)	Incl. (°)	Plat. (°)
10	5	83.1	303.2	355.3	39.3	22.3(N)
21	6	78.0	298.7	353.0	32.5	17.6
29	8	73.1	300.9	349.8	26.1	13.7
36	13	67.4	307.2	344.7	20.0	10.3
42	18	65.4	305.6	344.0	16.3	8.3
44	20	64.8	303.8	344.3	14.6	7.4
48	21	60.1	305.2	341.1	7.8	3.9
50	22	64.5	294.7	347.5	10.3	5.2
52	23	57.9	299.9	342.2	1.2	0.6
53	24	56.5	297.2	342.7	− 2.6	− 1.3(S)
55	25	54.6	293.6	343.7	− 7.8	− 3.9
57	26	52.4	292.3	343.5	−12.3	− 6.2
59	27	46.8	294.1	340.0	−20.9	−10.8
61	28	46.3	292.2	341.0	−22.7	−11.8
62	29	41.2	292.8	338.4	−30.3	−16.2
70	32	36.3	284.7	342.6	−40.6	−23.2
80	34	28.2	280.7	343.4	−51.2	−31.9
115**	R. T.	9.0	295.0	317.1	−61.8	−43.0

* After Klootwijk *et al.* (1985, Table 2c), based on data from India-Africa relative movement data with Africa fixed to hot spot reference frame.

** R. T. stands for Rajmahal Traps. Pole position is after Klootwijk and Radhakrishnamurthy (1981) with new age according to Baksi *et al.* (1988).

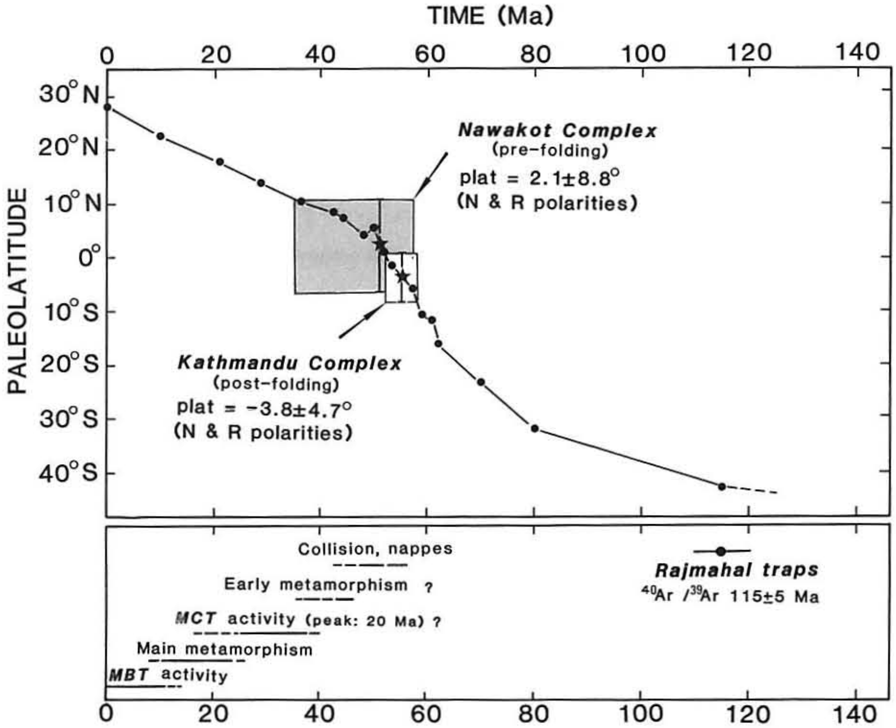

Text-fig. 12 Timing of the stable magnetic components. The upper diagram represents a paleolatitude-time plot for the present location of Malekhu based on data in Table 5. Dots are the expected paleolatitudes as a function of time. The mean paleolatitude estimates for the Nawakot and Kathmandu Complexes are plotted as stars with vertical uncertainty bars so as to yield time-paleolatitude boxes (finely dotted and open), respectively. The lower diagram shows the most probable age bars for various tectono-metamorphic events or processes according to various sources discussed in the text. Age of the Rajmahal traps is according to Baksi *et al.* (1988).

with respect to the Indian shield. An approximately 45° clockwise rotation was inferred previously when only limited data from the Nawakot Complex were available (Gautam and Yoshida, 1988). A better estimate of the minimum amount of the rotation made using the best site-mean direction (with smallest confidence angle) obtained in this study is 38±9° (Text-fig. 13).

Discussion

The stable magnetic components from the Nawakot and Kathmandu Complexes yielding shallow nearly-equatorial latitudes suggest the most probable acquisition time between 50 and 55Ma. The atable remanence in the Nawakot Complex was acquired mainly before folding but in the Kathmandu Complex after folding. Folding, nappe emplacement and metamorphism might have occurred during a short time span at the onset or the initial stage of the India-Eurasia collision or even

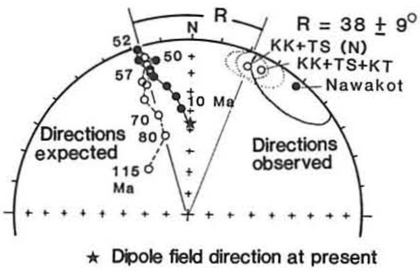

Text-fig. 13 Estimation of the inferred clockwise rotation of the Malekhu area relative to the Indian Shield.

shortly after the collision. The difference in magnetic history should probably be searched in the differences in thermal history in the two Complexes along other factors.

Treloar *et al.* (1989) determined hornblende and mica K/Ar and 40Ar/39Ar ages in the rocks of the former Indian plate segment in Pakistan Himalaya to range between 25 and 45Ma with a cluster around 30-35Ma and interpreted in terms of the simultaneous occurrence of deformation, heating, and metamorphism shortly after collision. They advocate the Himalayan-wide nature of the metamorphism which shortly postdated collision and bring to the attention 40Ar/39Ar data from eastern Garhwal (Hodges *et al.*, 1988) suggesting a pre-late Eocene early Barrovian metamorphism there.

In the High Himalaya, two metamorphic stages are thought to exist. The first metamorphic stage corresponds to the major eo-Himalayan or eo-MCT tectono-metamorphic moderately high pressure event which produced the regional fabric in the medium and upper part of the crystallines (Caby *et al.*, 1983; Pecher, 1989) and is reflected in the older cooling trajectory suggested to range from late Cretaceous to Eocene (Arita *et al.*, 1990). The second relatively low-pressure metamorphic stage is regarded as Miocene and equated to the pulses of granite emplacement dated to range from 25Ma to 15Ma (Deniel *et al.*, 1987) and is responsible for the younger post Eocene-Oligocene cooling trajectory of Arita *et al.* (1990). Hubbard and Harrison (1989) further determined 40Ar/39Ar ages on hornblende and mica and came to the conclusion that thrust movement and metamorphism in the MCT zone occurred ca. 21Ma and the granitic intrusion in the High Himalaya took place at the same time.

According to Le Fort (1989) the area under consideration represents one of the zones of " cold " thrusts, which correspond to the continuation in a more brittle domain of the MCT deformation. The transition from ductile to brittle accompanies a thrust climbing up section in the crust along the base of a wedge-shaped nappe. In this model, the Mahabharat thrust seems to be an extension of the MCT. Provided that the peak MCT activity took place around 21Ma, the time of the nappe emplacement would be Miocene or probably even younger.

Some of the age ranges for the tectono-metamorphic events/processes are shown in the lower section of Text-fig. 12 to seek the connection between the magnetic components observed and those events. The acquisition of the characteristic components seems to have related to some phenomena which occurred at the onset of the India-Eurasia collision. If proved to be true by further studies, it would mean that the tectonic activity and the deformation in the area covered by Lesser Himalayan crystallines might have occurred long before the peak MCT activity (accepted mainly as Miocene in the existing literature), and there may actually be no similarity between the MCT and MBhT. That the MCT functioning might have initiated at the onset of the collision also seems to be a possibility and should be studied in future.

The actual (regional or local?) significance of the $38\pm9°$ clockwise rotation of the Malekhu area relative to the Indian Shield may be established only when estimates of paleomagnetically derived rotations will be available from the neighbouring areas in the Lesser Himalaya. It is noteworthy, however, that similar magnitudes of rotations have been reported from the various parts of northwestern and central Himalayan region on the basis of observed secondary components, which have been dated at 50Ma to less than 60Ma and attributed to thermochemical effects associated with the initial India-Asia collision (Klootwijk *et al.,* 1985, 1986).

Conclusions

Major findings based on this paleomagnetic study can be summarized as follows:

a) Well-defined stable secondary components carried out by hematite are present in the metasediments. In the Kathmandu Complex rocks, the directions show NNE or SSW declination with almost horizontal inclination and exhibit good grouping before any tilt correction. In the Nawakot Complex rocks, however, better grouping of the directions foming the stable component is observed after tilt correction resulting also in NNE and SSW declination and shallow-inclination. The acquisition of the stable directions occurred at near-equatorial latitudes. Occurrence of major folding, nappe emplacement and metamorphism during a relatively long time span (probably several Myrs) is suggested to explain the occurrence of pre-folding and post-folding dual-polarity remanence of probably thermochemical origin. Such tectonometamorphic phenomena seem to be in close relation to the collision between India and Eurasia.

b) A minimum of $38\pm9°$ clockwise rotation of the Malekhu area with respect to the Indian shield since the early Tertiary time is inferred.

c) Minor *in situ* components, close to the present dipole field thought to be of recent and viscous origin are also observed.

Finally, it should be noted that further accumulation of paleomagnetic data and reliable ages from the Lesser Himalaya will assist in better time resolution of the components and better understanding of the tectono-metamorphic framework.

Acknowledgements

This work forms a part of research carried out during my doctoral studentship in the Hokkaido University. I express my sincere thanks to Prof. Dr. M. Kato, Dr. Y. Fujiwara and Dr. K. Arita (Department of Geology and Mineralogy, Hokkaido University) for their invaluable advices and comments on various occasions.

I am very much indebted to Dr. M. P. Sharma, Mr. M. R. Dhital, Mr. S. Panta and other colleagues in the Central Department of Geology, Tribhuvan University for their encouragement and/or kind support during the field work.

Receipt of the Monbusho (the Ministry of Education and Culture) scholarship from the Japanese Government is gratefully acknowledged.

References

Arita, K., Gautam, P. and Ganzawa, Y., 1990. Two metamorphic stages of the Nepal Himalayas prior and posterior to India-Eurasia collision. *Jour. Fac. Sci., Hokkaido Univ.*, ser. IV, 22 (4), *this volume.*

Baksi, A. K., Barman, T. R., Paul, D. K. and Farrer, E., 1987. Widespread Early Cretaceous flood basalt volcanism in eastern India: Geochemical data from the Rajmahal-Bengal -Sylhet Traps. *Chem. Geol.*, 63: 133-141.

Caby, R., Pecher, A. and Le Fort, P., 1983. Le grand chevauchement central Himalayen: nouvelles donnes sur le metamorphisme inverse a la base de la Dalle du Tibet. *Revue de Geographie physique et de Geologie Dynamique*, 24: 89-100.

Deniel, C., Vidal, C., Fernandes, A. and Le Fort, P., 1987. Age, origin and emplacement of an Himalayan leucogranite: the Manaslu example (Nepal). *Contr. Mineral. and Petrol.*, 96: 78-92.

Dunlop, D. J., 1972. Magnetic mineralogy of unheated and heated red sediments by coercivity spectrum analysis. *Geophys. J. R. astr. Soc.*, 27: 37-55.

Fisher, R. A., 1953. Dispersion on a sphere. *Proc. Royal Soc. London*, A, 217: 295-305.

Gautam, P., 1989. Magnetic properties of some late Paleozoic to Tertiary sedimentary rocks of Tansen area, Lesser Himalaya, Nepal. *Jour. Fac. Sci., Hokkaido Univ.*, ser. IV, 22(3): 467-487.

Gautam, P., 1990. Paleomagnetic study of the Lesser Himalaya in Nepal. Unpublished Doctoral thesis, Hokkaido University, Sapporo, Japan, 165+pp.

Gautam, P. and Yoshida, M., 1988. On the secondary magnetization observed in the Nawakot Complex rocks, Malekhu area, central Nepal. *Jour. Nepal Geol. Soc.*, v. 5(1): 1-10.

Hodges, K. V., Hubbard, M. S. and Silvergerg, D. S., 1988. Metamorphic constraints on the thermal evolution of the central Himalayan Orogen. *Phil. Trans. R. Soc. Lond.* A 326: 257 -280.

Hubbard, M. S. and Harrison, T. M., 1989. 40Ar/39Ar age constraints on deformation and metamorphism in the Main Central Thrust zone and Tibetan slab, eastern Nepal Himalaya. *Tectonics*, 8(4): 865-880.

Klootwijk, C. T., Conaghan, P. J. and Powell, C. McA., 1985. The Himalayan Arc: large-scale continental subduction, oroclinal bending and back-arc spreading, *Earth Planet. Sci. Lett.*, 75: 167-183.

Klootwijk, C. T., Sharma, M. L., Gergan, J., Shah, S. K. and Gupta, B. K., 1986. Rotational overthrusting of the northwestern Himalaya: further palaeomagnetic evidence from the Riasi thrust sheet, Jammu foothillis, India. *Earth Planet. Sci. Lett.*, 80: 375-393.

Klootwijk, C. T. and Radhakrishnamurthy, C., 1981 Phanerozoic palaeomagnetism of the Indian plate and the India-Asia collision. *In*: M. W. McElhinny and D. A. Valencio (eds), *Palaeoreconstruction of the continents*, Am. Geophys. Union. Geodynam. ser. 2: 93-105.

Le Fort, P., 1989. The Himalayan orogenic segment. *In*: A. M. C. Sengör (ed), *Tectonic Evolution of the Tethyan Region*, 289-386. Kluwer Academic Publishers.

Pecher, A., 1989. The metamorphism in the Central Himalaya. *J. metamorphic Geol.*, 7: 31-41.

Stöcklin, J., 1980. Geology of Nepal and its regional frame. *J. Geol. Soc. London,* 137: 1-34.

Stöcklin, J. and Bhatterai, K. D., 1980. Geological map of Kathmandu area and Central Mahabharat range, scale 1 : 250000, HMG Nepal.

Treloar, P. J., Rex, D. C., Guise, P. G., Coward, M. P., Searle, M. P., Windley, B. F., Petterson, M. G., Jan, M. Q. and Luff, I. W., 1989. K-Ar and Ar-Ar geochronology of the Himalayan collision in NW Pakistan: constraints on the timing of sututring, deformation, metamorphism and uplift. *Tectonics,* 8(4) : 881-909.

Zijderveld, J. D. A., 1967. A. C. demagnetization of rocks: analysis of results. *In :* D. W. Collinson, K. M. Creer and S. K. Runcorn (eds), *Methods in Paleomagnetism,* Elsevier, Amsterdam : 254-286.

(Manuscript received on Feb. 15, 1990 ; and accepted on Feb. 22, 1990).